JOURNAL OF
EMERGING INVESTIGATORS

Article

Linear relationship between nanostructural features and coloring of biomimetic photonic material

Muzi Dou[1], Nadia Abascal[1]
[1] Blair Academy, Blairstown, New Jersey

SUMMARY

Biomimetic photonic materials manipulate light in a way so that different colors of light reflect depending on the viewing angle, resulting in an iridescent effect. These materials are aesthetically pleasing and used in design; they have the potential to serve as a great resource for art if it is possible to manipulate and design them. Due to the seemingly unpredictable relationship between biomimetic photonic materials' nanostructural features and coloration, current research has not arrived upon a consistent method to engineer these materials to consistently achieve desired coloration. We hypothesized that in biomimetic photonic materials, there exists linear relationships between nanostructural features of iridescence and their coloring features. We collected data from previous studies in which researchers synthesized polystyrene core shell particles coated with melanin-like polydopamine shell layers (PSt@PDA materials), a type of biomimetic photonic material. Based on this data, we built a series of linear regression models in R that describe the relationships between PSt@PDA core shell particle diameter and the coloring features, including hue, saturation, and brightness, at all viewing angles and two lightings, and then developed a user-friendly interface to visualize the predicted color based on user-defined inputs. With these results, engineers should be able to precisely target nanostructural features that need to be changed in order to achieve a specific coloration.

INTRODUCTION

Biomimetic photonic materials are materials that reflect different colored light based on viewing angle (1). They often have robust mechanical strength, good wettability, and technical applications in chemical sensors, biosensors, active color display units, and printing, among others (2). Aside from its mechanical practicalities, these photonic materials have strong aesthetic potential. Animals with iridescent features such as butterflies, hawksbill turtles, and peacocks are largely sought after for fashion and décor. Biomimetically iridescent materials are also widely used in design of accessories, clothing, furniture, etc. Iridescent paints are made available to artists by very few sources, and are often considered to be very limited and expensive. The ability to predict the coloring of biomimetic photonic materials based on nanostructural inputs could allow the efficient design of biomimetic photonic materials. This ability aided by an easy-to-use visualization platform could allow very accessible customization of biomimetic photonic materials. However, due to complicated nanostructure of biomimetic photonic materials, this has yet to be done.

In previously published work, researchers have successfully synthesized polystyrene core shell particles (PSt) coated with melanin-like polydopamine (PDA) shell layers, also known as PSt@PDA particles, an example of biomimetic photonic materials with facile synthetization (3). They have collected visual data that results in the altering of nanostructural variables, and concluded that coloring of particles is mostly dependent on only two variables: diameter of PSt particles and concentration of PDA coating (3). However, they did not establish a quantitative connection between the altering of the nanostructural features and the resulting change in the particle coloring. This lack of a quantitative relationship between PSt@PDA material's nanostructure and coloration indicates that previous research cannot directly enable the design of PSt@PDA particles.

In this study, we hypothesized that there exists a quantitative relationship between PSt@PDA material's nanostructure and coloring. We treated PSt diameter and PDA coating concentration as independent variables and observed that they were quantitatively related to the dependent variable of material coloring. We were able to represent colors with the hue, saturation, and brightness (HSB) scale, where hue is the name of the color, saturation is how little white is mixed into the hue, and brightness is how little black is mixed into the hue. Through analyzing synthetization results of previous papers with Excel and R, we mapped a linear relationship between PSt@PDA core shell diameter and its hue at all viewing angles. We set out to present this information in an interactable visual interface, eliminating the convoluted typical guess-and-check method in biomimetic photonic material design. In the future, we aim to synthesize the material to test the validity of our model. This work would offer valuable insights for the rational design of iridescence for art materials, allowing the average consumer to access a wider range of aesthetic options on the market, and the particularly artistically inclined to access cheaper and more eccentric materials in artistic creation.

RESULTS

To gauge the quantitative relationship between PSt@PDA material's nanostructure and coloration, we referenced previous labs' synthetization of PSt@PDA materials (3). We decided on using the HSB color scale for a quantitative measurement of color, as it works better than alternatives such as the red, green, and blue (RGB) scale. This is because the hue value directly measures shifts in color with a numerical gradient, while RGB's values do not directly correspond to colors seen with the naked eye. We collected data on each pellet's combination of color, PSt diameter, and PDA concentration. To simplify the model, we assimilated PSt diameter and PDA concentration into one variable: overall PSt@PDA core shell diameter (size).

https://doi.org/10.59720/25-020

We then ran a linear regression program in R's ggplot to see if there was a relationship between the core shell diameter and coloring. Data extracted from parts of the pellet unexposed to direct lighting and data extracted from parts of the pellet exposed to direct lighting (highlighted) of the pellet were processed in separate categories to account for the additional variable of lighting. At each angle, a linear regression for coloring was run for hue, saturation, and brightness, individually. The linear regression produced two important outcomes: a line of best fit that describes the relationship between the particle size and coloring, and an R^2 value that describes how strong the relationship between the particle size and coloring is. We graphed the relationships between PSt@PDA particle size and hue (**Figure 1A**), saturation (**Figure 1B**), and brightness (**Figure 1C**). We analyzed data for relationships between PSt@PDA core shell diameter (x) and coloring (y) at all viewing angles.

At all angles and lighting, there was a strong correlation between PSt@PDA particle size and hue, as indicated by an average R^2 value of 0.93 and 0.86 (**Figure 1A, Table 1**). There was a weak correlation between particle size and saturation, with an average R^2 value of 0.34 and 0.25 (**Figure 1B, Table 1**). There seemed to be minimal to no correlation between particle size and brightness, as seen by a low average R^2 value of 0.03 and 0.15 (**Figure 1C, Table 1**). Our data gives the clear indication that as particle size increases, the hue gradually shifts from blue to warmer tones such as green, red, then purple.

To represent our regression results, we wrote a user-friendly visualization program that shows the predicted color based on input values so that predictions are easier to visualize. The program allowed input values for both diameter and concentration of PSt@PDA particles and described the outcome in the form of a colored pellet (**Figure 2**). As visualized in the side-by-side comparison, results were generally accurate in hue, with some discrepancies addressed in the discussion section (**Figure 3**).

DISCUSSION

While previous studies have managed to synthesize and pinpoint the advantages of biomimetic photonic materials, there is a need for methods to predict material coloring based on nanostructural inputs to enable precise and efficient design of biomimetic photonic materials (2, 3). The studies by Kawamura et al. used the resulting colors of PSt coated in PDA to show that a correlation between the diameter of PSt particles and concentration of PDA coating determines the particle's color (3). While this study was promising it stopped short of establishing a quantitative connection between PSt diameter and PDA concentration, something that we aimed to define in our study. In many ways, we think that such a predictive approach based on the quantitative connection between PSt particle diameter and concentration of PDA coating will aid artists and other craftsmen in more streamlined syntheses of iridescent materials. This tool will allow them to achieve the desired color and iridescent flip without the trial-and-error that is currently a requirement for making these materials. In the same way that ceramic glazes must be fired in order to know their true color, we hope that our predictive model gives those who desire iridescent materials of certain colors an example on which to operate.

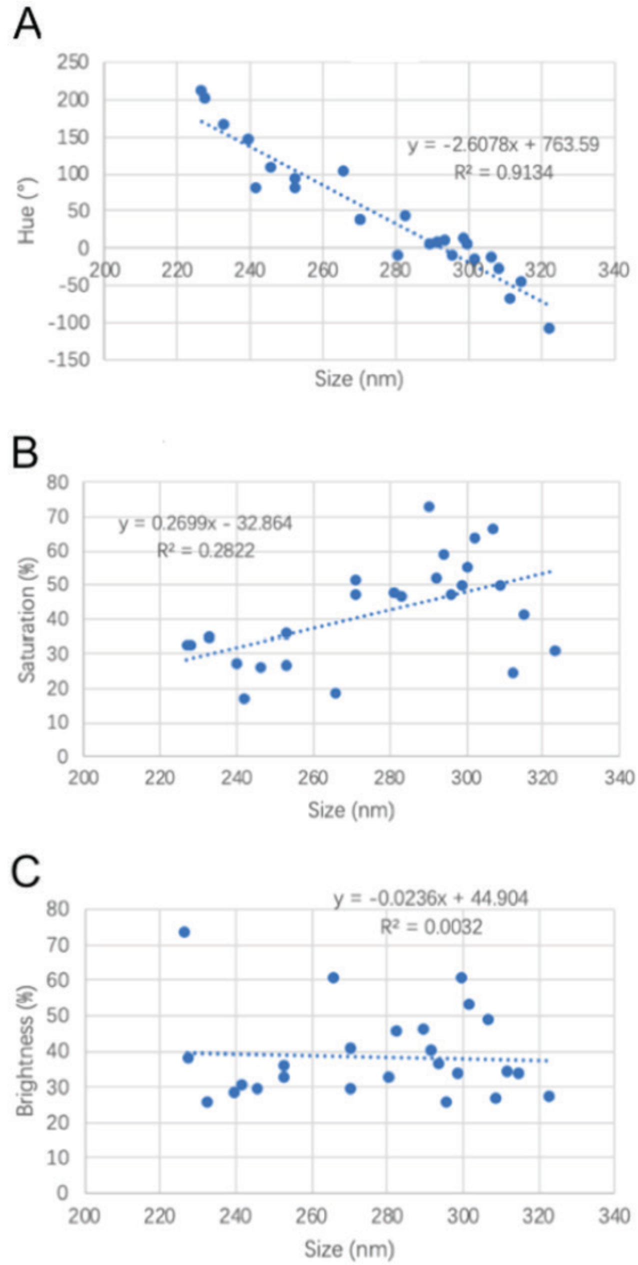

Figure 1: Examples of linear regression results relating several PSt@PDA coloration features to its particle size. Modeled relationships generated by Excel between PSt@PDA nanostructure and color at viewing angle of 90 degrees without direct light reflection to demonstrate the direction and strength of the relationships between PSt@PDA particle size and hue, saturation, and brightness. The modeled relationship between particle size and **A)** hue, **B)** saturation, or **C)** brightness.

Through the current work, we conclude that there exists a quantifiable relationship in PSt@PDA photonic materials' nanostructure and coloring. Specifically, we found that it is possible to integrate the PSt diameter and PDA concentration of PSt@PDA materials into one single variable: core shell diameter. Furthermore, PSt@PDA biomimetic photonic

https://doi.org/10.59720/25-020

Viewing angle (°)	Lighting condition	Hue		Saturation		Brightness	
		Equation	R^2	Equation	R^2	Equation	R^2
90	Not under direct light	y=-2.6x+764	0.91	y=0.27x-33	0.28	y=-0.02x+45	0.003
	Under direct light	y=-3.0x+871	0.93	y=0.32x-43	0.25	y=-0.17x+91	0.08
60	Not under direct light	y=-2.8x+819	0.94	y=0.35x-55	0.39	y=-0.04x+46	0.008
	Under direct light	y=-3.0x+886	0.88	y=0.16x+13	0.09	y=-0.05x+75	0.005
45	Not under direct light	y=-2.8x+832	0.93	y=0.36x-59	0.39	y=-0.03x+43	0.005
	Under direct light	y=-2.9x+863	0.84	y=0.33x-43	0.34	y=-0.35x+179	0.33
30	Not under direct light	y=-2.9x+856	0.93	y=0.32x-47	0.36	y=-0.06x+49	0.02
	Under direct light	y=-3.0x+882	0.81	y=0.33x-44	0.32	y=-0.33x+171	0.24
0	Not under direct light	y=-3.1x+905	0.92	y=0.25x-35	0.28	y=-0.12x+57	0.09
	Under direct light	y=-3.0x+894	0.84	y=0.27x-38	0.25	y=-0.24x+126	0.09
Average R^2	Not under direct light	-	0.93	-	0.34	-	0.03
	Under direct light	-	0.86	-	0.25	-	0.15

Table 1: Summary of Linear Regression Results. Modeled relationships between PSt@PDA nanostructure and hue, saturation, and brightness at all viewing angles in either indirect or direct lighting.

materials' core shell diameter has a clear and strong linear relationship with material hue. There is a weak but still linear relationship between core shell diameter and material saturation, while there is no relation at all between core shell diameter and material brightness. By integrating the quantitative relationship between core shell diameter and material coloring into a user-friendly program, our results can be visualized and used for design of PSt@PDA photonic materials. Currently, this model accepts continuous inputs for PSt values, and PDA values are limited to 0, 0.3, 0.5, 1.0, 1.5, and 2.0 mg/mL. This is due to our imperfect method of integrating PSt size and PDA concentration into a singular variable, particle size, presented earlier in the study.

There are several limitations to this study, including the fact that the PDA concentration values are limited. We have attempted fitting how PDA concentration affects PSt@PDA core shell diameter with linear, exponential, and polynomial regression, but those models do not adequately fit the data. We intend to perform multivariable regression to discover a trendline that represents how PDA concentration impacts PSt@PDA core shell diameter in order to integrate a continuous range for PDA concentration inputs in our

https://doi.org/10.59720/25-020

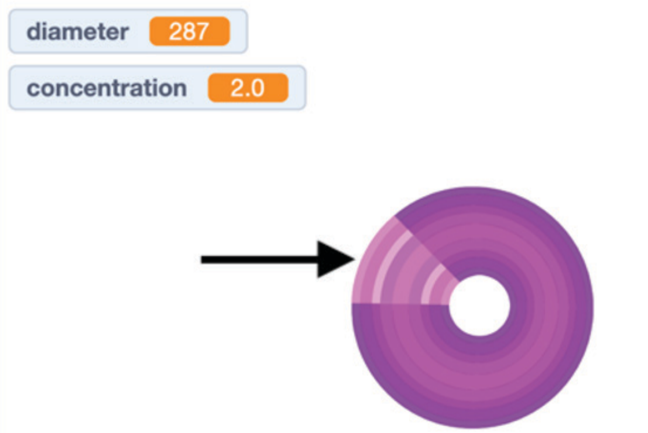

Figure 2: Visualization Platform. User-friendly visualization platform interface made with Scratch, a simple block coding program based on JavaScript. The program allows users to input a desired PSt diameter and a PDA concentration, generating a prediction for the color and iridescent shift. The example here shows that a PSt diameter of 287 nm and a PDA concentration of 2.0 mg/mL should produce a purple pellet with a pinkish iridescence (indicated by black arrow).

program. An additional limitation is that the specific domain and range of our model is unclear. Therefore, we are currently attempting Kawamura et al.'s method of synthesizing PSt@PDA materials to observe the bounds of which our model's predictions are valid. If successful, we hope to make the method of synthetization accessible as a method for taking advantage of PSt@PDA materials as an art medium.

Through this research, we discovered explicit quantifiable relationships between PSt@PDA materials' nanostructural features and coloration, and packaged it in a user-friendly program for designers. This takes us one step closer to efficient and accessible design of iridescent materials for artistic purposes.

MATERIALS AND METHODS

Data Source

Data was sourced from "Full-Color Biomimetic Photonic Materials with Iridescent and Non-Iridescent Structural Colors" (3). Data was collected by color-picking from each unit of synthesized PSt@PDA material pictured in Kawamura's results through Medibang Paint Pro. Pellets were color picked in regions not reflecting direct light at their highest point (viewing angle at 90 degrees), lowest point (viewing angle at 0 degrees), midpoint between the highest and lowest point (viewing angle at 45 degrees), and one and two-thirds points between the highest and lowest point (viewing angles at 60 and 30 degrees, respectively). This process was repeated for each pellet in its regions reflecting direct light. Medibang's RGB color format was converted to HSB through Rapidtables (4).

Data Processing

For each PDA value, we practiced linear regression of PSt diameter to particle size to compile PDA concentration and PSt diameter into one variable. A spreadsheet was generated for each particle size in correspondence to its HSB value. Linear regression was run for particle size in relation to hue, saturation, and brightness, respectively. Linear regression was conducted through Microsoft Excel's trendline function (**Appendix**) and R's ggplot2 package (5).

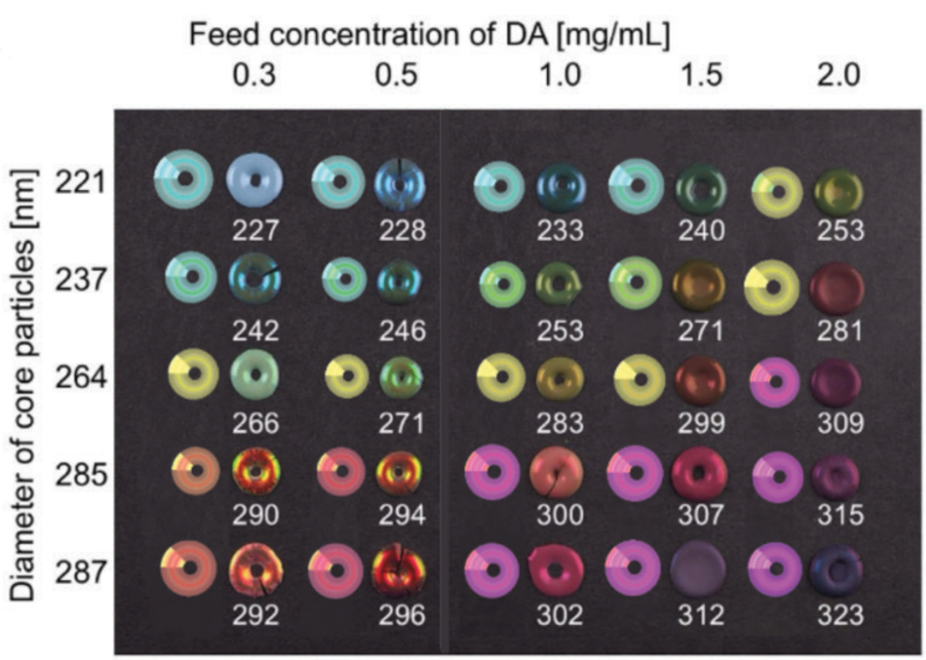

Figure 3: Visual Representation of Modeled Results. Recreation of a previously published figure by Kawamura et al. (3). The white numbers in the original image represent particle size. In addition to the previously published data, we included the predictions from our model generated by our visualization platform (left) to show a side-by-side comparison of our predictions of iridescence color with the iridescence color of real synthesized materials (right).

User-Interactable Interface

Scratch, a simple block coding program based on JavaScript, was used to create a user interactable interface. We used Scratch's built-in art tool to draw several rings indented within each other (**Figure 2**). For each ring, we uploaded the linear regression results from the corresponding angle with the particle size as a variable. The program then prompts the user for the desired PSt diameter and PDA concentration, and compiles the two variables into particle size to replace the variable. The program is then able to color in each ring with the predicted color based on particle size.

Received: October 29, 2024
Accepted: July 6, 2025
Published: April 24, 2026

REFERENCES

1. Whitney, Heather M., et al. "Flower Iridescence Increases Object Detection in the Insect Visual System without Compromising Object Identity." *Current Biology*, vol. 26, no. 6, Mar. 2016, pp. 802–808, https://doi.org/10.1016/j.cub.2016.01.026.
2. Xu, Jun and Zhiguang Guo. "Biomimetic Photonic Materials with Tunable Structural Colors." *Journal of Colloid and Interface Science*, vol. 406, Sep. 2013, pp. 1–17, https://doi.org/10.1016/j.jcis.2013.05.028.
3. Kawamura, Ayaka, et al. "Full-Color Biomimetic Photonic Materials with Iridescent and Non-Iridescent Structural Colors." *Scientific Reports*, vol. 6, no. 1, 23 Sept. 2016, https://doi.org/10.1038/srep33984.
4. "RGB to HSV color conversion." *RapidTables.com*, 2007, https://www.rapidtables.com/convert/color/rgb-to-hsv.html. Accessed 3 Sep 2024.
5. Wickham, Hadley. "Create Elegant Data Visualisations Using the Grammar of Graphics." *Tidyverse.org*, 2019, ggplot2.tidyverse.org/. https://ggplot2.tidyverse.org/reference/ggplot2-package.html.

Appendix

PSt Particles' Diameter [nm]	PDA Coating Concentration [mg/mL]	Core Shell Particle Diameter	Angle of Observation	Hue Without Light Reflection (deg)	Saturation Without Light Reflection (%)	Color Without Light Reflection (%)	Hue With Light Reflection (deg)	Saturation With Light Reflection (%)	Color With Light Reflection (%)	Iridescence
221	0.0	221	90	252	2.1	95.3	240	0.4	94.1	1
221	0.0	221	60	252	2.1	94.5	240	0.8	94.5	1
221	0.0	221	45	250	2.5	94.5	228	2	96.1	1
221	0.0	221	30	252	2.1	93.3	222	4	99.2	1
221	0.0	221	0	180	1.8	86.3	223	5.6	98.4	1
237	0.0	237	90	290	2.5	94.9	252	2.1	94.9	1
237	0.0	237	60	290	2.5	93.3	173	3.6	96.9	1
237	0.0	237	45	249	2.9	93.3	186	4	97.6	1
237	0.0	237	30	60	2.7	86.7	191	4.3	99.6	1
237	0.0	237	0	216	15.1	98.8	208	6	97.6	1
264	0.0	264	90	286	5.3	96.5	295	5.4	94.5	1
264	0.0	264	60	300	3.8	93.3	202	3.3	95.3	1
264	0.0	264	45	300	3.8	92.5	193	3.6	96.9	1
264	0.0	264	30	300	3.5	90.2	192	4	98.8	1
264	0.0	264	0	215	10.6	96.1	180	4.5	96.9	1
285	0.0	285	90	207	3.7	94.1	342	4.1	96.5	1
285	0.0	285	60	207	3.8	92.2	192	10.8	94.1	1
285	0.0	285	45	218	3.4	91	185	18.5	93.3	1
285	0.0	285	30	273	4.8	90.6	198	9.6	94.1	1
285	0.0	285	0	268	6	85.1	22	3.2	98.8	1
287	0.0	287	90	195	10	93.7	177	23.4	92.2	1
287	0.0	287	60	188	15.1	93.3	199	12.1	93.7	1
287	0.0	287	45	183	21.3	88.2	180	3.4	92.5	1
287	0.0	287	30	194	17.1	89.4	60	0.8	94.9	1
287	0.0	287	0	234	8.6	86.3	45	4.7	99.6	1
221	0.3	227	90	209	32.3	72.9	210	32.1	74.5	1
221	0.3	227	60	210	31.7	71.8	211	31.4	73.7	1

221	0.3	227	45	209	36.4	69	213	23.5	93.3	1
221	0.3	227	30	209	37.6	69.8	216	25.1	92.2	1
221	0.3	227	0	209	37.8	61.2	218	28.6	80.8	1
237	0.3	242	90	78	16.9	30.2	173	10.7	32.9	1
237	0.3	242	60	124	33.7	34.9	186	58.9	48.6	1
237	0.3	242	45	170	22.2	31.8	185	50.2	97.6	1
237	0.3	242	30	175	17.9	26.3	199	46.5	85.1	1
237	0.3	242	0	202	28.4	26.3	214	33.5	64.3	1
264	0.3	266	90	101	18.3	60	123	12.6	59.2	1
264	0.3	266	60	109	18.8	56.5	129	26.4	81.6	1
264	0.3	266	45	115	17.9	54.9	137	23.1	88.2	1
264	0.3	266	30	118	19.7	51.8	149	20.6	82	1
264	0.3	266	0	127	23.3	45.5	162	13.6	69.4	1
285	0.3	290	90	3	72.6	45.9	0	76.3	54.5	1
285	0.3	290	60	4	75.6	49.8	30	80.3	93.7	1
285	0.3	290	45	5	72.8	62	51	77.7	98.4	1
285	0.3	290	30	1	75.5	43.1	78	76.1	98.4	1
285	0.3	290	0	2	65.5	34.1	94	72.8	79.2	1
287	0.3	292	90	7	51.5	39.6	8	70.7	52.2	1
287	0.3	292	60	354	55.9	46.3	357	64.3	72.5	1
287	0.3	292	45	353	54.4	57.6	10	58.4	88.6	1
287	0.3	292	30	352	59.6	55.3	44	46	98	1
287	0.3	292	0	356	43	44.7	62	38.5	91.8	1
221	0.5	228	90	199	32.3	37.6	211	39	48.2	1
221	0.5	228	60	202	23.2	32.2	194	52	88.2	1
221	0.5	228	45	192	13.2	29.8	187	38.2	99.6	1
221	0.5	228	30	209	28.4	31.8	203	35.1	97.3	1
221	0.5	228	0	215	34.7	29.4	220	31.3	63.9	1
237	0.5	246	90	107	25.7	29	146	40.2	34.1	1
237	0.5	246	60	110	19	24.7	188	65.3	76.9	1
237	0.5	246	45	97	14.3	22	185	52.8	97.3	1
237	0.5	246	30	105	16	19.6	197	44.1	96.9	1
237	0.5	246	0	150	5.4	14.5	212	35	61.6	1
264	0.5	271	90	36	46.6	40.4	58	33.3	43.5	1
264	0.5	271	60	70	34.4	35.3	115	56.4	79.2	1
264	0.5	271	45	78	38.4	33.7	141	41	89.8	1

264	0.5	271	30	78	32.1	31.8	162	34.5	88.6	1
264	0.5	271	0	75	25	25.1	147	15.6	55.3	1
285	0.5	294	90	9	58.7	36.1	8	77.1	61.6	1
285	0.5	294	60	2	61	39.2	28	70.6	97.3	1
285	0.5	294	45	357	62.5	34.5	49	73	98.8	1
285	0.5	294	30	3	53.4	28.6	64	74.2	94.1	1
285	0.5	294	0	5	40	21.6	72	56.3	59.2	1
287	0.5	296	90	348	46.9	25.1	10	75.6	33.7	1
287	0.5	296	60	338	66.7	25.9	347	89.9	85.5	1
287	0.5	296	45	334	65.1	24.7	12	70.8	95.3	1
287	0.5	296	30	329	47.7	17.3	49	70.4	98	1
287	0.5	296	0	280	22.2	10.6	58	65.6	75.3	1
221	1.0	233	90	164	34.4	25.1	202	29.5	99.6	0
221	1.0	233	60	180	19	22.7	201	44.6	61.6	0
221	1.0	233	45	175	24.5	20.8	202	29.5	99.6	0
221	1.0	233	30	180	28.6	19.2	211	32.1	94.1	0
221	1.0	233	0	175	25.6	16.9	213	32.3	48.6	0
237	1.0	253	90	92	26.4	35.7	97	31.9	35.7	0
237	1.0	253	60	89	30.9	31.8	68	47.3	43.9	0
237	1.0	253	45	90	31.2	30.2	58	37.8	75.7	0
237	1.0	253	30	87	29	27.1	64	31	68.2	0
237	1.0	253	0	90	20.7	22.7	93	16.4	47.8	0
264	1.0	283	90	40	46.1	45.1	36	52.5	47.8	0
264	1.0	283	60	43	47.9	37.6	34	62.6	54.5	0
264	1.0	283	45	39	44.7	36.9	38	56	82	0
264	1.0	283	30	43	45.8	32.5	39	57.6	77.6	0
264	1.0	283	0	38	34.3	27.5	38	39	57.3	0
285	1.0	300	90	2	54.9	60	0	52.7	65.5	0
285	1.0	300	60	1	53.4	52.2	353	58.5	78.4	0
285	1.0	300	45	1	53.5	49.8	351	55.6	91	0
285	1.0	300	30	354	55	42.7	5	52.7	87.8	0
285	1.0	300	0	348	47	25.9	16	44.6	61.6	0
287	1.0	302	90	343	63.7	52.9	342	65.4	53.3	0
287	1.0	302	60	344	64.5	48.6	342	60.6	70.6	0
287	1.0	302	45	343	64.4	46.3	337	64.3	81.2	0
287	1.0	302	30	336	65.7	42.4	337	68.8	87.8	0

287	1.0	302	0	335	56.9	28.2	340	60.8	72.9	0
221	1.5	240	90	145	26.8	27.8	145	31	27.8	0
221	1.5	240	60	143	24.6	25.5	111	39.7	26.7	0
221	1.5	240	45	140	23.4	25.1	113	12.4	82.4	0
221	1.5	240	30	135	21.4	22	137	12.5	65.9	0
221	1.5	240	0	160	14.3	16.5	191	13.9	31	0
237	1.5	271	90	36	51.4	29	34	48.7	29.8	0
237	1.5	271	60	41	47.1	26.7	32	73.6	41.6	0
237	1.5	271	45	43	42.9	22	36	49.3	82	0
237	1.5	271	30	42	44.2	20.4	37	50.3	75.7	0
237	1.5	271	0	34	38.1	16.5	38	38.6	39.6	0
264	1.5	299	90	11	49.4	33.3	9	52.6	29.8	0
264	1.5	299	60	3	48.6	29	352	70.1	38	0
264	1.5	299	45	358	46.9	25.1	359	48.5	80	0
264	1.5	299	30	358	44.8	22.7	2	55.6	73.3	0
264	1.5	299	0	349	37.8	17.6	8	38.5	37.6	0
285	1.5	307	90	345	66.1	48.6	343	65.1	49.4	0
285	1.5	307	60	344	61.5	42.7	333	68	69.8	0
285	1.5	307	45	342	63.2	37.3	335	69.1	81.2	0
285	1.5	307	30	343	60	31.4	343	66.3	74.5	0
285	1.5	307	0	337	58.6	22.7	347	53.2	48.6	0
287	1.5	312	90	291	24.4	33.7	318	27.7	36.9	0
287	1.5	312	60	289	25.6	32.2	302	26.1	43.5	0
287	1.5	312	45	282	23.6	28.2	290	28.7	39.6	0
287	1.5	312	30	278	27.9	26.7	262	31.1	41.6	0
287	1.5	312	0	295	23.9	18	295	28.4	31.8	0
221	2.0	253	90	79	35.4	32.2	71	33.3	31.8	0
221	2.0	253	60	81	30.7	29.4	54	61.7	36.9	0
221	2.0	253	45	79	35.2	27.8	51	40.3	74.9	0
221	2.0	253	30	75	27.6	22.7	54	36.4	64.7	0
221	2.0	253	0	72	20.8	18.8	75	13.3	35.3	0
237	2.0	281	90	349	47.6	32.2	349	45.3	29.4	0
237	2.0	281	60	345	45.7	27.5	344	61.7	36.9	0
237	2.0	281	45	345	40.7	23.1	342	51.7	58.4	0
237	2.0	281	30	342	47.3	21.6	341	52.8	56.5	0
237	2.0	281	0	341	50	17.3	349	44.4	28.2	0

264	2.0	309	90	331	49.3	26.3	321	55.8	30.2	0
264	2.0	309	60	329	45.8	23.1	319	51.4	28.2	0
264	2.0	309	45	325	46.2	20.4	323	45.3	41.6	0
264	2.0	309	30	324	40	19.6	323	44.5	43.1	0
264	2.0	309	0	319	40	15.7	325	46.4	32.9	0
285	2.0	315	90	314	41.2	33.3	304	39.2	29	0
285	2.0	315	60	311	48.5	25.9	291	47.4	45.5	0
285	2.0	315	45	312	45.6	22.4	312	51.5	40.4	0
285	2.0	315	30	308	43.1	20	315	59.1	36.5	0
285	2.0	315	0	304	44.7	14.9	323	36.2	31.4	0
287	2.0	323	90	251	30.9	26.7	235	29.7	29	0
287	2.0	323	60	246	34.5	22.7	225	61.9	44.3	0
287	2.0	323	45	250	34	20.8	224	60.4	54.5	0
287	2.0	323	30	249	38	19.6	255	38.3	36.9	0
287	2.0	323	0	270	38.9	14.1	310	30.4	31	0